

# Thermodynamic phase structure of complex Sachdev-Ye-Kitaev model and charged black hole in deformed JT gravity

Sizheng Cao,<sup>1</sup> Yi-Cheng Rui,<sup>1</sup> and Xian-Hui Ge<sup>1,\*</sup>

<sup>1</sup>*Department of Physics, Shanghai University, Shanghai, 200444, China*

(Dated: March 31, 2021)

The van der Waals-Maxwell phase transition theory is among the oldest and the most simplest theories describing thermodynamic phase transitions in physics. Studying the complex Sachdev-Ye-Kitaev (cSYK) model numerically and deriving a new black hole solution in Jackiw-Teitelboim (JT) gravity analytically, we investigate how these models behave like the van der Waals-Maxwell liquid-gas model. The cSYK model exhibits first order phase transition terminating at the critical point, while the charged black hole in JT gravity shows a clear van der Waals-Maxwell like phase structure. In the absence of charge, the corresponding neutral black hole still has the Hawking-Page phase transition. The black hole solution also provides the first example in JT gravity yielding the van der Waals-Maxwell like phase structure.

*Introduction.*— As a concrete microscopic model with low energy holographic dual, the Sachdev-Ye-Kitaev (SYK) model, describing  $N$  Majorana fermions with random  $q$ -body interactions, has been the focus of much recent attention in both the quantum gravity and the condensed matter literature. The emergence of conformal symmetry, the  $AdS_2$  factor, the absence of quasi-particle excitations and the maximal chaos in the low temperature limit of the SYK model strongly indicates that the SYK model at finite temperature is dual to a black hole solution in two-dimensional JT gravity [1–4]. Recently, Maldacena and Qi (MQ) studied two statistically correlated copies of the SYK model with a bilinear coupling term [5]. This coupled SYK model (MQ model) has an interesting phase diagram at finite temperature, which demonstrates the Hawking-Page phase transition between the thermal AdS phase at low temperature and two black holes phase at high temperature. Another interesting aspect of this coupled SYK model is that a new phase emerges in the large  $q$  limit with a negative specific heat. Notably, the similar first-order phase transition was also observed in melonic quantum mechanics with  $U^2(n)$  symmetry [6, 7] and Yukawa-SYK model [8, 9]. The complex version of the MQ model was further studied in [10–12] and same Hawking-Page phase transition observed there, while no phase transition was observed in mass deformed single-sided SYK model [13].

The well-known Hawking-Page phase transition discovered in 1983 describes the phase transition between AdS thermal gas (unstable small black hole) to finite temperature neutral black hole (large black hole) in AdS spacetime [14]. Concerned the SYK/JT duality, it is significant to explore the Hawking-Page phase transition in the deformations of JT gravity. Very recently, Witten considered an arbitrary dilaton potential such that there are black hole solutions asymptotic at infinity to the nearly  $AdS_2$  solutions of the standard JT gravity and further showed that if there is a black hole solution at temperature  $T$  with negative specific heat, there will be

another black hole solution at the same temperature with a positive specific heat and lower free energy [15] (see also [16, 17]). There can be first-order phase transitions similar to the Hawking-Page transition between them. Nevertheless, there are richer thermodynamic phase structures for a class of charged black holes in AdS spacetime, including structures isomorphic to the van der Waals-Maxwell liquid-gas system [18, 19]. Compared with the Hawking-Page phase transition, the appearance of a stable small black hole solution is a new feature when one adds small fixed charge to the Schwarzschild-AdS black hole.

As long as the SYK model has a neutral black hole dual, one has strong motivations to investigate how the cSYK model behaves like a charged black hole in AdS spacetime [20]. This is not only because both of them have globally conserved charge, but also because they may share the same thermodynamic structure. Moreover, the microscopic structure of black holes can be better understood through obtaining an exact charged black hole solution in JT gravity which is dual to the cSYK model. The aim of this letter is to explore thermodynamic phase transition of cSYK model, present a new charged black hole solution in JT gravity yielding the Van der Waals-Maxwell-like thermodynamical phase structure, and compare these two models.

*The model and thermodynamics.*— The cSYK model of fermions is the charge conserving variant of the Majorana SYK model yielding the Hamiltonian

$$H = \sum_{i,j,k,l=1}^N J_{ijkl} c_i^\dagger c_j^\dagger c_k c_l - \mu \sum_i c_i^\dagger c_i, \quad (1)$$

where  $c_i, c_i^\dagger$  are fermion operators satisfying  $\{c_i, c_j^\dagger\} = \delta_{ij}$ . In the natural units, the model depends on the chemical potential  $\mu$  and the temperature  $T$ . The couplings  $J_{ijkl}$  are independent random complex Gaussian variables with zero mean and the following variance  $\overline{J_{ijkl}} = 0$ ,  $\overline{|J_{ijkl}|^2} = \frac{J^2}{8N^3}$ . We can define the global conserved  $U(1)$  charge by  $Q = \sum_i^N (c_i^\dagger c_i - \frac{1}{2})$ , which is related

to the ultraviolet (UV) asymmetry of the Green function  $G(\tau, \tau') = \langle T c_i(\tau) c_i^\dagger(\tau') \rangle$ ,  $G(0^-) = -\frac{1}{2} - \mathcal{Q}$ ,  $G(0^+) = \frac{1}{2} - \mathcal{Q}$ ,  $\mathcal{Q} = \frac{\langle \mathcal{Q} \rangle}{N}$ . In the infrared, the Green function is characterized by the long-time behavior of the Green function  $G_{\beta=\infty}(\pm\tau) \sim \mp e^{\pm\pi\mathcal{E}} \tau^{-1/2}$ ,  $\tau \gg J^{-1}$ . The parameter  $\mathcal{E}$  is the spectral asymmetry parameter controlling the particle-hole asymmetry. The asymmetry parameter  $\mathcal{E}$  is related to the thermodynamic residue entropy  $\mathcal{E} = \frac{1}{2\pi} \frac{\partial S_0}{\partial \mathcal{Q}}$ . This is an important property of both complex SYK and charged black holes with  $AdS_2$  horizons because in the holographic picture  $\mathcal{E}$  describes the electric field on the horizon [21, 22]. Through disorder averaging with keeping only replica-diagonal terms and integrating out the fermion fields, we find the general form of the effective action

$$-S_{\text{effective}} = \ln \det \left[ (\partial_\tau - \mu) - \Sigma \right] + \int d\tau d\tau' \left[ \Sigma(\tau, \tau') G(\tau', \tau) + \frac{J^2}{4} G^2(\tau, \tau') G^2(\tau', \tau) \right] \quad (2)$$

The corresponding Schwinger-Dyson equation is given by

$$G(i\omega_n) = \frac{1}{-i\omega_n - \mu - \Sigma}, \quad \Sigma(\tau) = -J^2 G^2(\tau) G(-\tau), \quad (3)$$

where  $\omega_n = (2n+1)\pi/\beta$  are Matsubara frequencies. We solve the Schwinger-Dyson equation numerically by iteration. The solution of  $G(\tau)$  satisfying the relation  $G(0^+) + G(0^-) = 1$  is computed for different temperatures and chemical potentials in the Supplemental Material, where one can find that a gap opens up at the low temperature in the presence of a chemical potential  $\mu$ . The free energy can be obtained by substituting the saddle point solutions into the effective action

$$\frac{F}{N} = -T \left[ \ln 2 + \frac{1}{2} \sum_{\omega_n} \ln \left( \frac{(-i\omega_n - \mu - \Sigma)^2}{-\omega_n^2} \right) + \frac{3}{4} \sum_{\omega_n} \Sigma(i\omega_n) G(i\omega_n) \right]. \quad (4)$$

The energy can be calculated as

$$\frac{E}{N} = \frac{1}{4} \left[ -4\mu \left( \mathcal{Q} + \frac{3}{4} \right) + \mu + T \sum_{\omega_n} \Sigma(i\omega_n) G(i\omega_n) \right]. \quad (5)$$

The phase diagram of this single sided cSYK model is dominated by the presence of a critical point  $(T_c, \mu_c) = (0.06828, 0.3443)$  as shown in figure 1(a). The large  $T$ , fixed  $\mu$  and large  $\mu$ , fixed  $T$  regions of the  $(\mu, T)$ -plane corresponds to the gapped weakly coupled fermion and gapless strongly correlated SYK phases, respectively. The large  $\mu$  regime describes a system of weakly interacting governed by the perturbative field theory, while the small  $\mu$  regime describes the strongly coupled system and has a black hole description. Varying the chemical potential allows us to study the phase transition between the weakly coupled regime and a strong coupled

black hole regime. The transition temperature  $T_c$  grows monotonously with  $\mu$  and terminates at the critical point  $(T_c, \mu_c)$ . In figure 1(b), we plot the free energy density as a function of temperature by sweeping from high to low temperatures, and vice versa. For high temperatures, the black hole phase is favored whereas for low temperatures the weakly coupled fermions prevails. We can observe a clear hysteresis between these two solutions, indicating a first-order phase transition ending at the critical point. As we cross over into the large charge regime at some critical value of  $\mu$ , the hysteresis disappears and the free energy becomes a simple monotonic function.

The evolution of the free energy of the system as a function of chemical potential is shown clearly as one goes from zero to large chemical potential as illustrated in figure 1(c). We can also observe that as the chemical potential increases and approaches the critical value  $\mu_c$ , the first-order phase transition occurs at higher temperature and eventually the kink in the free energy vanishes. For large chemical potential, there is only a single saddle point solution, meaning that the weakly coupled phase dominates. Such observations are also consistent with the  $\mu - \mathcal{Q}$  diagram as demonstrated in figure 1(d) in which the charge difference can be regarded as the order parameter. Note that below  $T_c$ , no saddle point solutions found for a range of  $\mathcal{Q}$  in the  $\mu - \mathcal{Q}$  diagram even in the large  $q$  limit. This missing portion corresponds to those that cannot be obtained numerically from a stable convergent iterative series which may be identified as the thermodynamically unstable branch with a negative specific heat. In the vicinity of the critical point, we can calculate the critical exponents as shown in table I following [7]. The definition of the critical exponents comes from the specific heat  $c(T, \mu_c) = T \frac{\partial S}{\partial T} \propto |T - T_c|^{-\alpha_\pm}$ , the charge susceptibility  $\chi(T, \mu_c) = \frac{\partial \mathcal{Q}}{\partial \mu} \propto |T - T_c|^{-\gamma_\pm}$ , the charge density as a function of temperature  $|\mathcal{Q}(T, \mu_c) - \mathcal{Q}(T_c, \mu_c)| \propto |T - T_c|^{q_\pm}$ , the charge difference between two phases  $\Delta \mathcal{Q} \propto |T - T_c|^{\beta_c}$ , the entropy as a function of chemical potential  $|S(T_c, \mu) - S(T_c, \mu_c)| \propto |\mu - \mu_c|^{s_\pm}$  and the charge density as a function of  $\mu$   $|\mathcal{Q}(T_c, \mu) - \mathcal{Q}(T_c, \mu_c)| \propto |\mu - \mu_c|^{\tilde{q}_\pm}$ , where  $\alpha_+$  denotes  $\alpha$  computed above critical point ( $T > T_c$ ) and  $\alpha_-$  denotes  $\alpha$  computed below critical point ( $T < T_c$ ), and the same for  $\gamma_\pm, q_\pm, s_\pm, \tilde{q}_\pm$ . The non-mean field theory exponents obtained here indicate that the cSYK model seems to work as a statistically microscopic model of the traditional liquid-gas phase transition.

*Charged black hole solution*— Now we move to a possible mean field theory description of the phase structure of cSYK model from the JT gravity. We first derive the black hole solution and study its thermodynamic phase structure. We consider the 2D JT gravity with a Maxwell

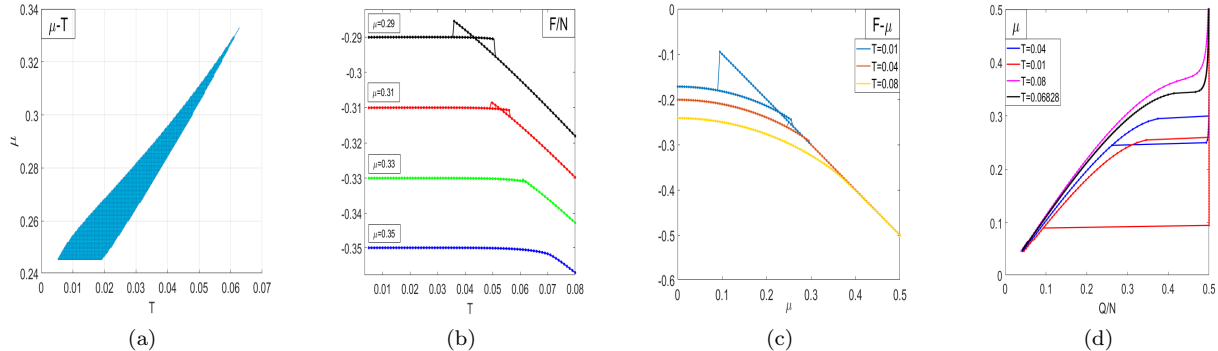


FIG. 1: (a) The chemical potential as a function of  $T$ , obtained by calculating the free energy hysteresis curves for different values of  $\mu$ . The shaded region indicates the parameter range where the phases coexist. (b) The free energy as a function of temperature for different values of  $\mu$ . We decrease temperature from high temperature to low temperature, and then increase back. The hysteresis indicates a first-order phase transition as two solutions cross. As the chemical potential increases, the hysteresis region shrinks, indicating the system is approaching the critical points. (c) The free energy as a function of chemical potential for different values of temperature. As temperature increases, the hysteresis appears which signaling the first-order phase transition. (d) The chemical potential as a function of the charge density for different  $T$ . For  $T < T_c$ , there are two distinct solutions one SYK and another weakly coupled fermions. For  $T = T_c$ , there is a single solution with a singular behavior at  $\mu = \mu_c$ . For  $T > T_c$ , the  $\mu(Q)$  curve is smooth.

TABLE I: Critical exponents

$\alpha_+$	0.6388	$\alpha_-$	0.6644
$\gamma_+$	0.5815	$\gamma_-$	0.7537
$q_+$	0.4007	$q_-$	0.4714
$s_+$	0.5202	$s_-$	0.4224
$\tilde{q}_+$	0.5116	$\tilde{q}_-$	0.4265
$\beta_c$	0.6397		

field as

$$\begin{aligned}
S_{\text{JT}}^{\text{charg}} &= \frac{\phi_0}{2} \left( \int_{\mathcal{M}} d^2x \sqrt{-g} R + 2 \int_{\partial\mathcal{M}} \sqrt{-h} K d\tau \right) \\
&+ \frac{1}{2} \int_{\mathcal{M}} d^2x \sqrt{-g} \left( \phi R + \frac{V(\phi)}{l^2} - \frac{1}{2} Z(\phi) \mathcal{F}^2 \right) \\
&+ \frac{1}{2} \int_{\partial\mathcal{M}} d\tau \sqrt{-h} K_\mu Z(\phi) \mathcal{F}^{\mu\nu} \mathcal{A}_\nu + \int_{\partial\mathcal{M}} \sqrt{-h} \phi K d\tau \\
&+ \int_{\partial\mathcal{M}} \sqrt{-h} \mathcal{L}_{\text{ct}} d\tau. \tag{6}
\end{aligned}$$

where  $l$  is the AdS radius,  $K$  is the extrinsic curvature,  $K_\mu$  a unit normal vector and  $\mathcal{L}_{\text{ct}}$  a boundary counter term that keeps the on-shell action finite. The terms in the first bracket in the action are topological and independent of the dilaton field  $\phi$ . Multiplying by a constant  $\phi_0$ , they do not contribute to the equation of motion but the sum is proportional to a topological invariant, the Euler character of the 1 + 1-dimensional manifold. Remarkably, the Maxwell field is included in the action which can make the black hole charged so that the resulted black hole solution may behave as the Reinsser-Nordström-AdS black holes with rich phase structures.

Nevertheless, as proved in [23, 24], charged black holes in JT gravity in a canonical ensemble with fixed charge correspond to neutral black holes with a proper choice of the dilaton potential, which is called the charged/neutral black hole duality [25].

After solving the equations of motion, we can obtain the charged black hole solution

$$\begin{aligned}
ds^2 &= -f(r)dt^2 + \frac{dr^2}{f(r)}, \tag{7} \\
\phi(r) &= r, \quad V(\phi(r)) = 2r + \frac{a_0}{r^\eta}, \\
f(r) &= \frac{r^2 - r_H^2}{l^2} + \frac{a_0}{(1-\eta)l^2} \left( r^{1-\eta} - r_H^{1-\eta} \right) \\
&\quad - \frac{\mathcal{Q}^2}{(1-\zeta)l^2} \left( r^{1-\zeta} - r_H^{1-\zeta} \right), \\
Z(\phi) &= r^\zeta, \quad \mathcal{A}_t(r) = \mu + \frac{\mathcal{Q}}{1-\zeta} r^{1-\zeta},
\end{aligned}$$

where the dilaton potential is chosen to satisfy  $V(\phi_\infty) = 2r$  for  $r \rightarrow \infty$  and  $a_0$  is a constant parameter with  $a_0 > 0$ . The exponents  $\eta$  and  $\zeta$  are also assumed to be positive with  $\eta > \zeta > 0$ . The event horizon locates at  $r = r_H$  and the chemical potential is given by  $\mu = \frac{\mathcal{Q}}{\zeta-1} r_H^{1-\zeta}$ . The general discussions on the JT gravity black hole solutions and their deformations can be found in [15, 23, 24].

Because of the charged/neutral black hole duality, one can also obtain a neutral version of black hole solution by choosing the dilaton potential as  $V(\phi(r)) = 2r + \frac{a_0}{r^\eta} - \frac{b_0}{r^\zeta}$ . The equivalent neutral action without Maxwell field

reads

$$\begin{aligned}
S_{\text{JT}}^{\text{neut}} &= \frac{\phi_0}{2} \left( \int_{\mathcal{M}} d^2x \sqrt{-g} R + 2 \int_{\partial\mathcal{M}} \sqrt{-h} K d\tau \right) \\
&+ \frac{1}{2} \int_{\mathcal{M}} d^2x \sqrt{-g} \left( \phi R + \frac{V(\phi)}{l^2} \right) + \int_{\partial\mathcal{M}} \sqrt{-h} \phi K d\tau \\
&+ \int_{\partial\mathcal{M}} \sqrt{-h} \mathcal{L}_{\text{ct}} d\tau. \tag{8}
\end{aligned}$$

The dilaton potential and the blacken factor become

$$\begin{aligned}
V(\phi) &= 2r + \frac{a_0}{r^\eta} - \frac{b_0}{r^\zeta}, \tag{9} \\
f(r) &= \frac{r^2 - r_H^2}{l^2} + \frac{a_0}{(1-\eta)l^2} \left( r^{1-\eta} - r_H^{1-\eta} \right) \\
&- \frac{b_0}{(1-\zeta)l^2} \left( r^{1-\zeta} - r_H^{1-\zeta} \right).
\end{aligned}$$

By identifying  $b_0 = \mathcal{Q}^2$ , one can find that the metric given in (7) equals to (9). Hence, a proper choice of the dilaton potential  $V(\phi)$  for neutral black hole corresponds to the charged one in a canonical ensemble with fixed charge [26]. The blacken factor  $f(r)$  recovers the black hole solution in the standard JT gravity  $f(r) = \frac{1}{l^2}(r^2 - r_H^2)$  as  $a_0 = b_0 = \mathcal{Q}^2 = 0$ . The black hole thermodynamics is discussed in the Supplemental Material. The ADM mass can be identified as  $M = \frac{1}{2}r_H^2 + \frac{a_0}{2(1-\eta)}r_H^{1-\eta} - \frac{b_0}{2(1-\zeta)}r_H^{1-\zeta}$ . Hereafter, we mainly considered the charged black hole solution in canonical ensemble with  $a_0 = 1$ ,  $b_0 = \mathcal{Q}^2$ ,  $\eta = 1$ ,  $\zeta = 2$  and  $l = 1$ , particularly in plotting the figures.

*Thermodynamic phase structure.*—Intriguingly, such a 2D charged black hole solution can reproduce almost all the thermodynamic properties of the global RN-AdS black hole in higher dimensions. Defining the Euclidean signature  $t \rightarrow i\tau$  and identifying the period  $\beta$  of the imaginary time with the inverse temperature, one obtains

$$\beta = \frac{4\pi r_H^\zeta}{2r_H^{\zeta+1} + a_0 r_H^{\zeta-\eta} - b_0}. \tag{10}$$

This equation can be regarded as the equation of state, explicitly  $\beta = \beta(r_H, b_0)$ . The qualitative features of  $\beta(r_H)$  for varying  $b_0$  are illustrated in figure 2(a). The  $\beta(r_H)$  curve is analogous to the graph of the  $P(V)$  van der Waals equation of state, where the pressure  $P$  is replaced by  $\beta$  and the volume  $V$  by  $r_H$ . For different temperatures, we also plot the chemical potential as a function of the charge density, as illustrated in figure 2(b). Above the critical temperature, a first-order phase transition in the  $\mu - \mathcal{Q}$  occurs with the semicircle-like region corresponds to the missing portion in the cSYK model (the semi-circle like curve in cSYK can be found in [27]). Although the complete analogy between charged black hole and van der Waals liquid-gas phase transition can be established by treating the cosmological constant as

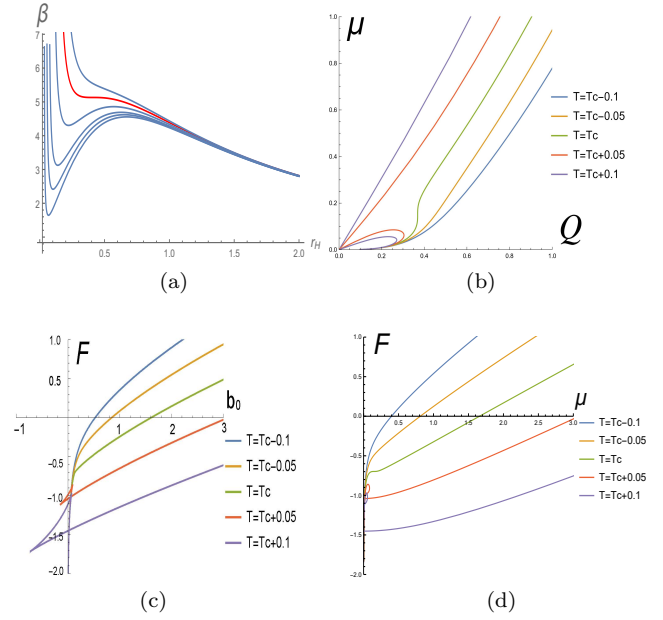


FIG. 2: (a) A family of isocharge curves for the  $(\beta, r_H)$  form of the equation of state. The red line is for the critical value of  $b_0 = \mathcal{Q}^2$ , below which multiple branches of  $r_H$  solutions appear. The vicinity of the critical point is a universal cubic for arbitrary positive  $\eta$  and  $\zeta$ . (b)  $\mu$  versus  $\mathcal{Q}$  for different  $T$  in the vicinity of the thermal critical point. The semicircle-like lines delimit the region where solutions are unstable. (c) The free energy  $F$  as a function of the squared charge density  $b_0 = \mathcal{Q}^2$ , where the swallowtail structure is shown explicitly. (d) The free energy  $F$  as a function of the chemical potential.

a pressure  $P = 1/4\pi l^2$  and the horizon radius as the specific volume [28–30], we would like to focus on (10) and leave the discussion on the case cosmological constant as the pressure in the future work. There is a critical value,  $b_{0,\text{crit}}$  below which there are three branches of black hole solutions for a range of values of  $\beta$ , corresponding to the small, middle and large black holes. As shown in table II, the existence of the critical values of  $r_H$ ,  $b_0$  and  $\beta$  is quiet universal for different values of  $\eta$  and  $\zeta$ . Note that for large  $r_H$ ,  $\beta$  goes as  $\sim 1/r_H$ . One may also notice that as  $\beta$  diverges, the denominator of  $\beta$  given by  $2r_H^{\zeta+1} + a_0 r_H^{\zeta-\eta} - b_0 = 0$ , has a single positive root  $r_e$ , which corresponds to the extremal black hole configuration with the zero temperature  $T = 0$ . Due to above facts, any turning points between  $r_e$  and  $r_H \rightarrow \infty$  must appear in pairs. The condition  $\partial\beta/\partial r_H = 0$  indicates that there are only two real, positive such solutions obeying the equation  $2r_H^{\zeta+1} - a_0 r_H^{\zeta-\eta} + b_0 \zeta = 0$ . These two solutions coalesce at the critical point  $\partial^2\beta/\partial^2 r_H = 0$  where  $b_0 = b_{0,\text{crit}}$ . The value of the radius of such critical black hole is  $r_{H,\text{crit}}$  and it is at inverse temperature  $\beta_{\text{crit}}$ . One can introduce  $\hat{b} = \frac{b_0}{b_{0,\text{crit}}}$ ,  $\hat{r}_H = \frac{r_H}{r_{H,\text{crit}}}$  and  $\hat{\beta} = \frac{\beta}{\beta_{\text{crit}}} = \frac{1}{T}$  and recast the equation of state (10) in a

$\eta, \zeta$	$r_{H,\text{crit}}$	$b_{0,\text{crit}}$	$\beta_{\text{crit}}$
$\eta = 1.2, \zeta = 1.5$	0.30	0.49	6.80
$\eta = 1, \zeta = 2$	$\frac{1}{\sqrt{6}}$	$\frac{1}{3\sqrt{6}}$	$2\sqrt{\frac{2}{3}}\pi$
$\eta = 1, \zeta = 3$	$\frac{1}{2}$	$\frac{1}{24}$	$\frac{3}{2}\pi$
$\eta = 2, \zeta = 3$	0.63	0.31	4.97
$\eta = 2, \zeta = 4$	0.74	0.16	4.55

TABLE II: The critical values of  $\{r_{H,\text{crit}}, b_{0,\text{crit}}, \beta_{\text{crit}}\}$  for different  $\eta$  and  $\zeta$  where we choose  $a_0 = 1$ .

dimensionless form

$$\hat{b} = 3\hat{r}_H + \hat{r}_H^3 - 3\hat{T}\hat{r}_H^2, \quad (11)$$

where we have set  $\eta = 1, \zeta = 2$  and  $a_0 = 1$ . The critical point locates at  $(\hat{T}_{\text{crit}}, \hat{b}_{\text{crit}}, \hat{r}_{H,\text{crit}}) = (1, 1, 1)$ . In the neighbourhood of the critical point, we can write  $\rho' = \hat{r}_H - 1, T' = \hat{T} - 1$  and  $P' = \hat{b} - 1$ , take  $(\rho', T')$  to be small and rewrite the equation of state as

$$P' = -3T' + \rho'^3 - 3\rho'^2T' - 6\rho'T' + \mathcal{O}(\rho'^2T', T'^2), \quad (12)$$

where  $\rho'$  can be regarded as the order parameter and  $T'$  the reduced temperature. At the critical temperature  $\hat{T} = 1$ , we obtain  $P' \sim \rho'^3$  from which one can extract the critical exponent  $\delta = 3$ . Near the critical point  $P' = -3T'$ , thus we have  $\rho' \propto (T')^{\frac{1}{2}}$  which means  $\beta = \frac{1}{2}$ . The susceptibility  $\chi$  is defined as  $\chi = (\frac{\partial \rho'}{\partial P'})_T$ ,

$$\chi = \frac{1}{3\rho'^2 - 6\rho'T' - 6T'}, \quad (13)$$

which indicates  $\chi \propto T'^{-1}$  when  $\rho' = 0$ , that is,  $\gamma = 1$ . Note that this critical exponent is universal because performing this computation for other values of parameters  $\eta, \zeta$  will not change the exponent. Equation (12) can be considered as the derivation of  $\rho'$  from the Landau-Ginzburg free energy

$$\hat{F} = \frac{1}{4}\rho'^4 + 3\rho'^2T' + (1 + 3T')\rho'. \quad (14)$$

Therefore, this basically is a kind of mean field theory and the corresponding critical exponents should be the same as that of mean field theory. In the canonical ensemble, the free energy in general is given by (see the Supplemental Material)

$$F = -\frac{1}{2}r_H^2 - \frac{b_0}{2}r_H^{-1} - \frac{1}{2} + \frac{1}{2}\ln r_H. \quad (15)$$

It can be observed that a plot of  $F(b_0)$  for fixed  $T$  above  $T_c$  exhibits a swallowtail structure, as shown in figure 2(c). To compare with the  $F-\mu$  diagram of cSYK model, we also draw the free energy as a function of chemical potential in figure 2(d). Different from the cSYK model, the first-order phase transition here happens at the temperature above  $T_c$ , but this is the same as that of RN-AdS black hole.

*Conclusions and discussions.*—In summary, we studied the thermodynamic phase structures of the microscopic complex SYK model and its possible gravity dual—the charged black holes in JT gravity. On the cSYK side, the free energy-temperature diagram shows a hysteresis structure, demonstrating a first-order phase transition ending at the critical point, analogous to the water-vapor transition. To compare with such a complex SYK model on the  $0+1$ -dimensional field theory side, we provide a 2D charged black hole solution in deformed JT gravity, yielding the familiar van der Waals-Maxwell-like phase structure. First-order phase transition is the common feature of both sides, but cSYK model provides microscopic description with non-mean field critical exponents to the water-vapor phase transition diagram, while the black hole model offers the mean field theory picture.

Unlike the  $\mu - Q$  diagram of the cSYK model, the isothermal curves for the  $\mu - Q$  diagram on the black hole side exhibit inverse dependence of the charge density. That is to say, as the charge density decreases below the critical value, phase transition occurs for black holes. For special case with  $b_0 = Q^2 = 0$ , the black hole thermodynamics phase diagram reduces to the Hawking-Page phase transition.

Interestingly, such a black hole solution can reproduce almost all the physical picture of global RN-AdS black holes with similar thermodynamic phase structure. This may help us understand the microscopic structure of black holes since it has a cSYK dual. Considered the related studies on the competition between chaotic and nonchaotic phases [31–33], it would be interesting to investigate the Lyapunov exponent for this charged black hole solution and compare the result with that of cSYK.

*Acknowledgement.*— We would like to thank Jinwu Ye, Pengfei Zhang, Shao-Kai Jian, Tian-Gang Zhou and Shao-Feng Wu for helpful discussions. This work is partly supported by NSFC, China (No.11875184).

\* Electronic address: gexh@shu.edu.cn

- [1] S. Sachdev and J. Ye, Phys. Rev. Lett. **70** (1993) 3339 [cond-mat/9212030].
- [2] A. Kitaev, A simple model of quantum holography, talks at KITP, 7 April 2015 and 27 May 2015.
- [3] J. Maldacena and D. Stanford, Phys. Rev. **D 94**, 106002 (2016).
- [4] K. Jensen, Phys. Rev. Lett. **117**, 111601(2016).
- [5] J. Maldacena and X. Qi, (2018) [arXiv:1804.00491[hep-th]].
- [6] T. Azeyanagi, F. Ferrari and F. I. S. Massolo, Phys. Rev. Lett. **120**, 061602 (2018).
- [7] F. Ferrari and F. I. S. Massolo, Phys. Rev. D **100** 026007 (2019).
- [8] Y. Wang and A. V. Chubukov, Phys. Rev. Research **2**, 033084 (2020).
- [9] W. Wang, A. Davis, G. Pan, Y. Wang and Z. Y. Meng,

- [arXiv:2102.10755[hep-th]].
- [10] S. Sahoo, E. Lantagne-Hurtubise, S. Plugge and M. Franz, Phys. Rev. Research **2** 043049 (2020). [arXiv:2006.06019[hep-th]].
- [11] T.-G. Zhou and P. Zhang, Phys. Rev. B **102**, 224305 (2020).
- [12] T.-G. Zhou, L. Pan, Y. Chen, P. Zhang, H. Zhai, [arXiv:2009.00277].
- [13] T. Nosaka and T. Numasawa, JHEP **08** 081 (2020).
- [14] S. W. Hawking and D. N. Page, Commun. Math. Phys. **87** 577 (1983).
- [15] E. Witten, [arXiv:2006.03494[hep-th]].
- [16] S. Sachdev, J. Math. Phys. **60** 5 052303 (2019).
- [17] A. Lala, H. Rathi and D. Roychowdhury, Phys. Rev. D **102**, 104024 (2020).
- [18] A. Chamblin, R. Emparan, C. V. Johnson and R. C. Myers, Phys.Rev. **D 60** 064018 (1999).
- [19] A. Chamblin, R. Emparan, C. V. Johnson and R. C. Myers, Phys. Rev. **D 60** 104026 (1999) [arXiv:hep-th/9904197].
- [20] Note that for the original SYK model, it does not show a Hawking-Page phase transition. This is different from the global Schwarzschild-AdS black hole which in the low temperature has a first order phase transition.
- [21] R. A. Davison, W. Fu, A. Georges, Y. Gu, K. Jensen and S. Sachdev, Phys. Rev. **B 95** 155131 (2017).
- [22] Y. Gu, A. Kitaev, S. Sachdev and G. Tarnopolsky, JHEP **02** 157 (2020).
- [23] D. Grumiller and R. McNees, JHEP **04** 074 (2007).
- [24] R. G. Cai, S. He, S.-J. Wang and Y.-X. Zhang, JHEP **2008** 102 (2020).
- [25] We would like to thank Song He for figuring out this point.
- [26] According to the charge/neutral duality of black hole solutions in deformed JT gravity, the  $a_0$  term can also be interpreted as a charged term stemmed from the  $U(1)$  gauge field.
- [27] M. Tikhonovskaya, H. Guo, S. Sachdev and G. Tarnopolsky, Phys. Rev. B **103**, 075141 (2021).
- [28] B. P. Dolan, Class. Quant. Grav. **28**, 125020 (2011), [arXiv:1008.5023[gr-qc]].
- [29] D. Kubiznak and R. B. Mann, JHEP **1207**, 033 (2012), [arXiv:1205.0559[hep-th]].
- [30] S.-W. Wei and Y.-X. Liu, Phys. Rev. Lett. **115** 111302 (2015).
- [31] Y.-X. Yu, J. Ye and C. L. Zhang, [arXiv:1903.02947[hep-th]].
- [32] A. M. Garcia-Garcia, B. Loureiro, Phys. Rev. Lett. **120**, 241603 (2018).
- [33] X. Chen, R. Fan, Y. Chen, H. Zhai and P. Zhang, Phys. Rev. Lett. **119** (2017) 207603.

---

## SUPPLEMENTAL MATERIAL

### A. Solving Schwinger-Dyson equations numerically

The effective action is given by

$$-\frac{S_{\text{effective}}}{N} = \ln \text{Det} \left[ (\partial_\tau - \mu)\delta - \Sigma \right] + \int d\tau d\tau' \left[ \Sigma(\tau, \tau')G(\tau', \tau) + \frac{J^2}{4}G^2(\tau, \tau')G^2(\tau', \tau) \right]. \quad (\text{S1})$$

The time translation invariance of Euclidean correlators  $G(\tau, \tau') = G(\tau - \tau')$  allow us recast the action as

$$-\frac{S_{\text{eff}}}{N} = \ln \text{Det} \left[ (\partial_\tau - \mu)\delta - \Sigma \right] + \beta \int d\tau \left[ \Sigma(\tau)G(-\tau) + \frac{J^2}{4}G^2(\tau)G^2(-\tau) \right]. \quad (\text{S2})$$

Utilizing the Fourier transformation

$$f(\tau) = \frac{1}{\beta} \sum_{\omega_n} e^{-i\omega_n \tau} f(i\omega_n), \quad f(i\omega_n) = \int_0^\beta d\tau e^{i\omega_n \tau} f(\tau), \quad (\text{S3})$$

we obtain the action

$$-\frac{S_{\text{eff}}}{N} = \ln 2 + \sum_{\omega_n} \frac{1}{2} \ln \left( \frac{-i\omega_n - \mu - \Sigma(i\omega_n)}{-i\omega_n} \right)^2 + \frac{3}{4} \sum_{\omega_n} \Sigma(i\omega_n)G(i\omega_n). \quad (\text{S4})$$

Considering [1], we renormalized determinant term by the fact  $\sum_{\omega_n} \ln(i\omega_n) = \ln 2$  to converge the series, which can correctly reproduce the partition function of  $N$  noninteracting complex fermion. The equations of motion from  $S_{\text{eff}}$  satisfy

$$\frac{\delta S_{\text{eff}}(G, \Sigma)}{\delta \Sigma(i\omega_n)} = 0, \quad \frac{\delta S_{\text{eff}}(G, \Sigma)}{\delta G(\tau)} = 0, \quad (\text{S5})$$

from which we can derive the corresponding saddle point equation, i.e. the Schwinger-Dyson equation

$$G(i\omega_n) = \frac{1}{-i\omega_n - \mu - \Sigma(i\omega_n)}, \quad \Sigma(\tau) = -J^2 G^2(\tau)G(-\tau). \quad (\text{S6})$$

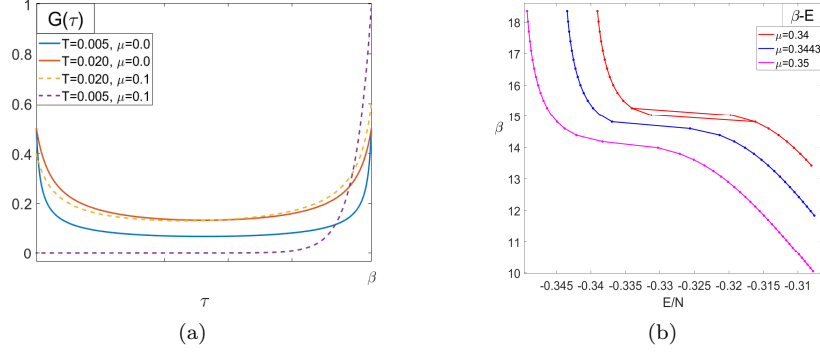


FIG. S1: (a) Numerical solution of  $G(\tau)$  for different temperatures and chemical potentials. The calculations are done for  $J = 1$  and  $q = 4$  and  $\Lambda = 2 \times 10^{17}$ . (b) The inverse temperature as a function of the energy for values of chemical potential below, equal and above  $\mu_c$ , respectively.

To find the solution for the Schwinger-Dyson equation above, one needs to solve the fixed-point equation as the form  $G(i\omega_n) = f(G(i\omega_n))$ , in this paper we are using the algorithm introduced in [1] and numerically calculate the solution for SD equation. Starting with an assumption for correlator and after a standard numerical procedure, the algorithm can always iterative out another solution by

$$G^{\text{new}}(i\omega_n) = (1 - x)G^{\text{prev}}(i\omega_n) + x \frac{1}{-i\omega_n - \mu - \Sigma(i\omega_n)}, \quad (\text{S7})$$

where we choose  $x = 0.05$  as the update parameter. At the same time, to initial the iteration we assume the noninteracting solution  $G(\tau) = \frac{1}{2}\text{sgn}(\tau)$  to be the solution for green function in the first round iterative procedure, and the coupling strength  $J$  set to be one. For numerical needs, we discrete the Euclidean time and the Matsubara frequency as

$$\tau_m = \frac{\beta m}{2\Lambda}, \quad (m = 0, 1, \dots, 2\Lambda - 1) \quad \text{and} \quad \omega_n = \frac{2\pi}{\beta}(\omega_n + \frac{1}{2}), \quad (n = -\Lambda, -\Lambda + 1, \dots, \Lambda - 1), \quad (\text{S8})$$

which is equivalent to introduce a UV cutoff, and for accuracy, most of the time we choose  $\Lambda = 2^{16}$ . After the final iteration is completed, one should evaluate the difference

$$\Delta G = \frac{1}{\Lambda} \sum_{\omega_n} |G^{\text{new}}(i\omega_n) - G^{\text{prev}}(i\omega_n)|. \quad (\text{S9})$$

When the difference is below a tolerance limits  $\Delta G < \epsilon = 10^{-14}$ , the algorithm will terminate the iteration. We thus can argue the numerical solution for Green function at this moment has converged. The numerical solution of the Green function  $G(\tau)$  at different temperatures and chemical potentials is shown in figure S1(a). Note that even in the zero temperature limit, the first-order phase transition exists as shown in figure S??. Figure S1(b) shows the inverse temperature as a function of the energy, which can be compared with the  $\beta - r_H$  diagram of charged black holes.

## B. Thermodynamic quantities of cSYK model

Once we obtain the numerical solution for Euclidean Green function, the energy can be expressed as a functional of Green function. Here we follow the way in [2] to obtain the expression of energy. First note that

$$N \partial_{\tau_1} G(\tau_1, \tau_2) \Big|_{\tau_1 - \tau_2 = 0^+} = N \partial_{\tau_1} G(\tau_1 - \tau_2) \Big|_{\tau_1 - \tau_2 = 0^+} = \sum_i \partial_{\tau} \langle c_i(\tau) c_i^\dagger \rangle = \sum_m \langle [H, c_m] c_m^\dagger \rangle, \quad (\text{S10})$$

where the Hamiltonian is given by

$$H = H_{\text{SYK}} + H_0 = \sum_{ij;kl} J_{ij;kl} c_i^\dagger c_j^\dagger c_k c_l - \mu \sum_i c_i^\dagger c_i. \quad (\text{S11})$$

After calculating the commutator  $[H, c_m]$  and insert the result into (S10), we have

$$N\partial_\tau G(\tau)|_{\tau=0^+} = \langle qH_{\text{SYK}} + H_0 \rangle, \quad (\text{S12})$$

with some additional terms, we can obtain the relation between Green functions and energy

$$N\partial_\tau G(\tau)|_{\tau=0^+} - \mu(q-1)\langle Q + \frac{N}{2} \rangle = \langle qH_{\text{SYK}} + H_0 + (q-1)H_0 \rangle = q\langle H \rangle, \quad (\text{S13})$$

which means the average energy is

$$\frac{E}{N} = \frac{1}{q} \left[ \partial_\tau G(\tau)|_{\tau=0^+} - \mu(q-1)\left(Q + \frac{1}{2}\right) \right], \quad (\text{S14})$$

where  $Q$  is the  $U(1)$  conserved charge density satisfying the relation

$$Q \equiv \frac{Q}{N} = -\frac{1}{2}[G(0^+) + G(0^-)]. \quad (\text{S15})$$

For the purpose of numerical calculations, we need to evaluate the first term in (S14). First, the saddle-point equation in our model is

$$(\partial_\tau - \mu)G(\tau) - \int_0^\beta \Sigma(\tau - \tilde{\tau})G(\tilde{\tau})d\tilde{\tau} = -\delta_\beta(\tau), \quad (\text{S16})$$

which means

$$\partial_\tau G(\tau) = \mu G(\tau) + \int_0^\beta \Sigma(\tau - \tilde{\tau})G(\tilde{\tau})d\tilde{\tau} + \delta_\beta(\tau). \quad (\text{S17})$$

Taking the limit  $\tau \rightarrow 0^+$  and using the expression for  $Q$ , we have

$$\partial_\tau G(\tau)|_{\tau=0^+} = \mu\left(\frac{1}{2} - Q\right) + \frac{1}{\beta} \sum_{\omega_n} \Sigma(i\omega_n)G(i\omega_n). \quad (\text{S18})$$

Finally we obtain the numerical computable formula for the energy

$$\frac{E}{N} = \frac{1}{q} \left[ 4\mu T \sum_{\omega_n} \text{Re}[G(i\omega_n)] - \mu + T \sum_{\omega_n} \Sigma(i\omega_n)G(i\omega_n) \right], \quad (\text{S19})$$

where we used the Dirichlet trick to ensure that the series converges

$$Q = -\frac{1}{2}[G(0^+) + G(0^-)] = -T \sum_{\omega_n} \text{Re}[G(i\omega_n)]. \quad (\text{S20})$$

After substituting the saddle point solution in (S4) we obtain the free energy

$$\frac{F}{N} = -T \left[ \ln 2 + \sum_{\omega_n} \frac{1}{2} \ln \left( \frac{-i\omega_n - \mu - \Sigma(i\omega_n)}{-i\omega_n} \right)^2 + \frac{3}{4} \sum_{\omega_n} \Sigma(i\omega_n)G(i\omega_n) \right]. \quad (\text{S21})$$

### C. Critical exponents in the vicinity of the critical point

In this subsection, we numerically compute the critical exponents near the critical point. The free energy  $F$  can also be evaluated from the effective action

$$\frac{F}{N} = -T \left[ \ln 2 + \frac{3}{4} \sum_{\omega_n} \Sigma(i\omega_n)G(i\omega_n) + \sum_{\omega_n} \frac{1}{2} \ln \left( \frac{-i\omega_n - \mu - \Sigma(i\omega_n)}{-\omega_n^2} \right)^2 \right]. \quad (\text{S22})$$

The entropy can be obtained from  $\frac{S}{N} = \frac{E-F}{NT}$ . These formulae for thermodynamic functions are valid when  $\mu > 0.25$  (see figure S2). When  $\mu < 0.23$ , these formulae lead to a diverge entropy at zero temperature. One can obtain two branches of the thermodynamic functions while increasing and decreasing  $T/\mu$  with fixed  $\mu/T$ .

The thermodynamic functions are sensitive to  $\mu$  and  $T$  near the critical points  $(\mu_c, T_c)$ . One can get the critical points by the following steps:



1. Set  $\mu = 0.34$  (any  $\mu$  with a first-order phase transition) and factor= 1.
2. Compute the free energy  $F$  at the highest temperature( $T = 0.1$ ) according to Green function. The Green function is initially set to be  $G(\tau) = 0.5$ .
3. Decrease the temperature by a step( $T_{\text{step}} = 10^{-5}$ ). Taking the Green's function obtained in the last step as the initial value, iterate to get the new Green function. Compute the free energy  $F$  at the new temperature.
4. Repeat step 3 until  $T = 0.005$ . We can obtain the free energy  $F_-$  as a function of temperature with fixed  $\mu$ .
5. Use the same method to get  $F_+$  by increasing the temperature from  $T = 0.005$  to  $T = 0.1$ .
6. If  $\max(|F_+(T) - F_-(T)|) < 10^{-9}$ , add factor  $\cdot \max(|F_+(T) - F_-(T)|)$  to  $\mu$  and multiply  $\mu$  by 1.1. If  $\max(|F_+(T) - F_-(T)|) \leq 10^{-9}$ , multiply  $\mu$  by 0.5.
7. Repeat step 2 to 6 until  $10^{-9} < \max(|F_+(T) - F_-(T)|) < 1.5 * 10^{-9}$ .
8. One can get  $\mu_c = \mu$ ;  $T_c$  is the temperature where  $F_+(T)$  have its largest absolute value of second derivative.

At the critical point, the temperature and the chemical potential takes the values  $T_c = 0.06828$  and  $\mu_c = 0.3443$ . We use the definition of critical exponent as follows [7]. The specific heat

$$c(T, \mu_c) = T \frac{\partial S}{\partial T} \propto |T - T_c|^{-\alpha_{\pm}}. \quad (\text{S23})$$

The charge susceptability

$$\chi(T, \mu_c) = \frac{\partial Q}{\partial \mu} \propto |T - T_c|^{-\gamma_{\pm}}. \quad (\text{S24})$$

The charge density difference as a function of temperature

$$|\mathcal{Q}(T, \mu_c) - \mathcal{Q}(T_c, \mu_c)| \propto |T - T_c|^{q_{\pm}}. \quad (\text{S25})$$

The charge density difference between two phases

$$\Delta \mathcal{Q} \propto |T - T_c|^{\beta_c}. \quad (\text{S26})$$

The entropy as a function of chemical potential

$$|S(T_c, \mu) - S(T_c, \mu_c)| \propto |\mu - \mu_c|^{s_{\pm}}. \quad (\text{S27})$$

The charge density as a function of the chemical potential

$$|\mathcal{Q}(T_c, \mu) - \mathcal{Q}(T_c, \mu_c)| \propto |\mu - \mu_c|^{\tilde{q}_{\pm}}, \quad (\text{S28})$$

where  $\alpha_+$  means  $\alpha$  computed above critical point( $T > T_c$ ) and  $\alpha_-$  means  $\alpha$  computed below critical point( $T < T_c$ ), and the same for  $\gamma_{\pm}, q_{\pm}, s_{\pm}, \tilde{q}_{\pm}$ . One can compute  $\Delta \mathcal{Q}$  in (S26) by the following steps:

1. Set  $T < T_c$ .
2. Compute the two branches of  $F - \mu$  and  $\mathcal{Q} - \mu$  relation with fixed  $T$ .
3. Find  $\mu_i$ , such that two branches of  $F - \mu$  intersect at  $\mu = \mu_i$ . The first-order phase transition occurs at  $\mu = \mu_i$ .
4.  $\Delta \mathcal{Q}(T) = |\mathcal{Q}_{\text{increasing}\mu}(\mu_i) - \mathcal{Q}_{\text{decreasing}\mu}(\mu_i)|$  at fixed T
5. Change  $T$  and repeat step 2 to 4. Finally get a  $\Delta \mathcal{Q} - T$  relation

They are not well-defined critical exponents because the exponents on two sides does not equal to each other [7].

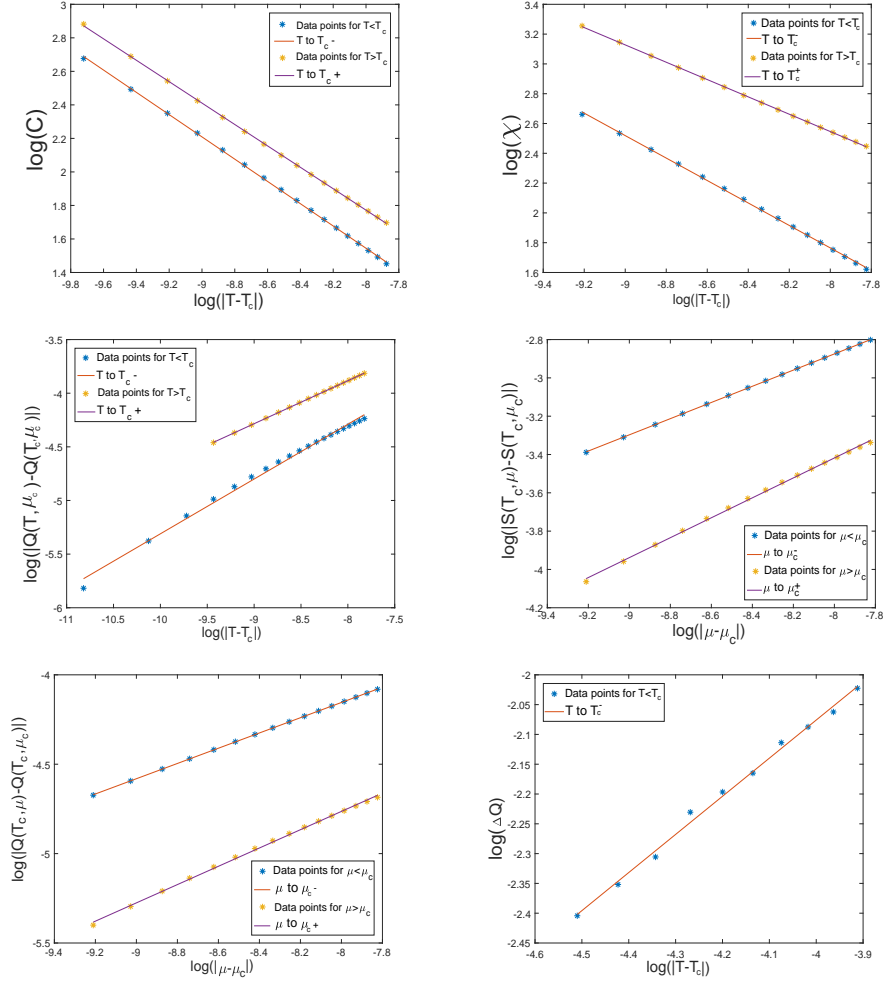


FIG. S2: Behaviors of thermodynamic functions near the critical point.

#### D. Black hole thermodynamics in deformed JT gravity

In this section, we briefly review the black hole thermodynamics for the deformed JT gravity. Related discussions can also be found in [3, 4]. We start with the bulk action in Euclidean signature

$$\begin{aligned}
S_{JT}^E &= S_{\text{top}}^E + S_{\text{bulk}}^E + S_{\text{GHY}}^E + S_{\text{ct}}^E \\
&= -\frac{\phi_0}{2} \left( \int_{\mathcal{M}} d^2x \sqrt{g} R + 2 \int_{\partial M} \sqrt{h} K d\tau \right) - \frac{1}{2} \int_{\mathcal{M}} d^2x \sqrt{g} \left( \phi R + \frac{V(\phi)}{l^2} - \frac{1}{2} Z(\phi) \mathcal{F}^2 \right) \\
&\quad - \int_{\partial M} \sqrt{h} \phi K d\tau + \int_{\partial M} \sqrt{h} \mathcal{L}_{\text{ct}} d\tau,
\end{aligned}$$

where  $h = f(r_\infty)$  is the induced metric and  $K$  is the extrinsic curvature of the boundary, explicitly  $K = \frac{f'(r_\infty)}{2\sqrt{f(r_\infty)}}$ . The  $\phi_0$  terms in the action (S29) are generated from the dimension reduction of the RN black hole and  $\phi_0 = Q_{\text{rn}}^2/2$  with  $Q_{\text{rn}}$  the charge of RN black hole. Considered the fact that

$$\lim_{\phi \rightarrow \infty} \int^{\phi} \left( \frac{V(\phi')}{l^2} - \frac{1}{2} Z(\phi) F^2 \right) d\phi' \rightarrow \infty, \quad (\text{S29})$$

the boundary counter term  $\mathcal{L}_{\text{ct}}$  should be of the form

$$\mathcal{L}_{\text{ct}}(\phi) = \sqrt{\frac{r^2}{l^2} - Q^2} + \frac{Q^2 r}{\sqrt{|f(\phi)|}}. \quad (\text{S30})$$

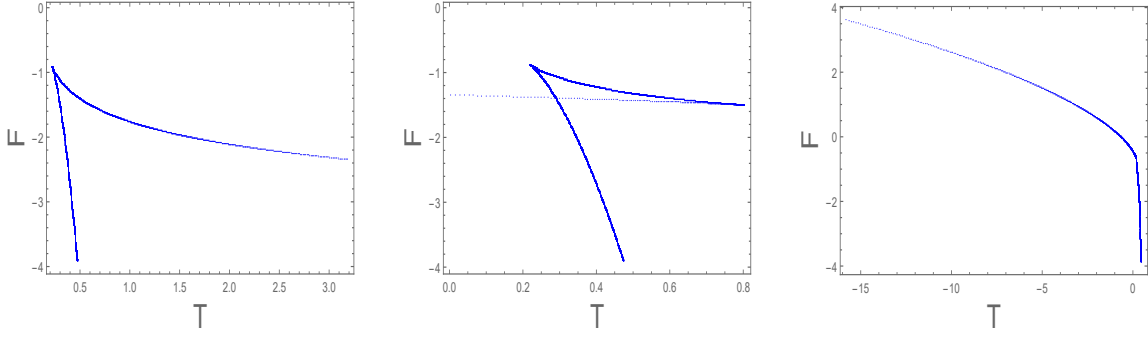


FIG. S3: The free energy as a function of temperature for the fixed charge ensemble for values  $b_0 = \mathcal{Q}^2 = 0$ ,  $b_0 = \mathcal{Q}^2 = 0.025$  and  $b_0 = \mathcal{Q}^2 = 0.149$  from left to right. Note that  $b_{0,\text{crit}} = 0.136$ , so in the right figure, the bend is in the vicinity of the critical point of second order.

The bulk on-shell action can be evaluated as

$$\begin{aligned}
S_{\text{bulk}}^E &= -\frac{1}{2} \int d^2x \sqrt{g} \left( \phi R + \frac{V(\phi)}{l^2} - \frac{1}{2} Z(\phi) \mathcal{F}^2 \right) \\
&= -\int d^2x \sqrt{g} \left( -\frac{\phi V'(\phi)}{2l^2} + \frac{V(\phi)}{l^2} + \frac{\mathcal{Q}^2}{2Z(\phi)} \right) \\
&= \frac{\beta \phi V(\phi)}{2l^2} \Big|_{\phi_H}^{\phi_\infty} - \beta J(\phi) \Big|_{\phi_H}^{\phi_\infty} - \frac{1}{2} \frac{\beta \mathcal{Q}^2 \phi}{Z(\phi)} \Big|_{\phi_H}^{\phi_\infty},
\end{aligned} \tag{S31}$$

where  $J(\phi) = \int \frac{V(\phi)}{l^2} d\phi$ . The Gibbons-Hawking-York term can be evaluated as

$$\begin{aligned}
S_{\text{GHY}}^E &= -\int \sqrt{h} \phi K d\tau = -\frac{\beta}{2} \phi(r_\infty) \left( \frac{V(r_\infty)}{l^2} - \frac{\mathcal{Q}^2}{Z(\phi_\infty)} \right) \\
&= -\frac{\beta \phi_\infty V(\phi_\infty)}{2l^2} + \frac{\beta \phi_\infty \mathcal{Q}^2}{2Z(\phi_\infty)}.
\end{aligned} \tag{S32}$$

The counter term reads

$$S_{\text{ct}}^E = \int_{\partial\mathcal{M}} \sqrt{h} \mathcal{L}_{\text{ct}} d\tau = -\beta M + \beta J(\phi_\infty), \tag{S33}$$

where the mass  $M$  is defined as  $M = J(\phi_H)/2$ . The total on-shell action is then given by

$$S_{\text{on-shell}}^E = S_{\text{bulk}}^E + S_{\text{GHY}}^E + S_{\text{ct}}^E = -\beta M + \beta J(\phi_H) - \frac{\beta \phi_H V(\phi_H)}{2l^2} + \frac{\beta \mathcal{Q}^2 \phi_H}{2Z(\phi_H)}. \tag{S34}$$

The free energy can be read off from the on-shell action

$$F = \frac{S_{\text{on-shell}}}{\beta} = M - \frac{\phi_H V(\phi_H)}{2l^2} + \frac{\mathcal{Q}^2 \phi_H}{2Z(\phi_H)}. \tag{S35}$$

The Hawking temperature and the entropy of the black hole are thus given by

$$\begin{aligned}
T &= \frac{f'(r_H)}{4\pi} = \frac{1}{4\pi l^2} \left( V(r_H) - \frac{\mathcal{Q}^2 l^2}{Z(\phi_H)} \right), \\
S &= 2\pi \phi_H.
\end{aligned} \tag{S36}$$

The  $\phi_0$  terms contribute to the entropy in the form as  $S = 2\pi(\phi_H + \phi_0)$ . The free energy  $F$  obeys the Euler relation

$$F = M - TS - \mu \mathcal{Q}, \tag{S37}$$

The first law of neutral black hole thermodynamics can be derived from the relation  $M = \frac{J(\phi_H)}{2}$  for  $q = 0$

$$\frac{dM}{dr_H} = \frac{V(\phi_H)}{2}, \quad V(\phi_H) = 4\pi T, \quad S = 2\pi\phi_H. \quad (\text{S38})$$

It is easy to obtain the first law of black hole thermodynamics  $dM = TdS$ . For charged black hole, the first law of thermodynamics becomes  $dM = TdS + \mu dQ$ .

For the metric obtained in this paper, the free energy can be written as

$$F = -\frac{1}{2}r_H^2 - \frac{b_0}{2}r_H^{-1} - \frac{1}{2} + \frac{1}{2}\ln r_H. \quad (\text{S39})$$

Note that we take values  $a_0 = 1$ ,  $\eta = 1$ ,  $\zeta = 2$  and  $l = 1$ . In general, the free energy can be expressed as

$$F = -\frac{1}{2}r_H^2 + \frac{a_0}{2}\frac{\eta}{1-\eta}r_H^{1-\eta} + \frac{b_0}{2}\frac{\zeta}{1-\zeta}r_H^{1-\zeta}. \quad (\text{S40})$$

The free energy as a function of temperature for the fixed charge ensemble is illustrated in Figure S3. The cusp structure can be observed for  $b_0$  indicates there is a first order phase transition, while as  $b_0$  increases, the swallowtail shape appears. Near the critical point, the curve approaches that of the second order.

---

\* Electronic address: gexh@shu.edu.cn

- [1] J. Maldacena and D. Stanford, Phys. Rev. **D 94**, 106002 (2016).
- [2] J. Maldacena and X. Qi, (2018) [arXiv:1804.00491[hep-th]].
- [3] E. Witten, [arXiv:2006.03494[hep-th]].
- [4] R. G. Cai, S. He, S.-J. Wang and Y.-X. Zhang, JHEP **2008** 102 (2020).